Velocity profiles in a real vegetated channel

Ludovic Cassan[1] · Gilles Belaud [2] · Jean Pierre Baume [2] · Cyril Dejean [2] · Frederic Moulin[1]

Abstract Most of the studies regarding vegetation effects on velocity profiles are based on laboratory experiments. The main focus of this paper is to show how the laboratory knowledge established for submerged vegetation applies to real scale systems affected by vegetation growth (mainly *Ranunculus fluitans*). To do so, experiments are conducted at two gage stations of an operational irrigation system. The analysis of first and second order fluctuations of velocities is based on field measurements performed by micro a coustic doppler velocimeter during 8 months, completed with flow measurement cam paigns in different seasons. The Reynolds stresses are used to determine shear velocities and deflected plant heights. Then, the modified log wake law (MLWL), initially derived from laboratory flume experiments, is applied with a unique parametrisation for the whole set of velocity profiles. The MLWL, along with a lateral distribution function, is used to calculate the discharge and to show the influence of vegetation height on the stage discharge relationships.

Keywords Open channel · Vegetation · ADV measurements · Rating curve

1 Introduction

In open channels, vegetation is known to affect flow properties such as roughness, as defined in head loss equations (e.g., Manning equation) or velocity profiles. Its influence must therefore be taken into account in many practical applications such as discharge estimation using rating curves, flow level prediction, pollutant dispersion, or the dynamics of sediment deposition. Most of the investigations related to vegetation effects have been

✉ Ludovic Cassan
lcassan@imft.fr

[1] Institut de Mecanique des Fluides, Allée du Prof. Camille Soula, 31400 Toulouse, France

[2] UMR G EAU, 361 Rue Jean Francois Breton, 34196 Montpellier, France

conducted in laboratory flumes where accurate experimental techniques can be used, such as micro acoustic doppler velocimeter (ADV) and particle image velocimetry (PIV). They have led to a better understanding of fundamental phenomena, such as turbulence forces induced by vegetation [25], or the effects of plant strength and foliage, as well as the development of predictive models of velocity profiles [2, 9, 22].

In natural streams, the complexity is increased due to many factors: heterogeneity of plant species, difficulty in characterizing plant characteristics, plant distribution within sections, three dimensional effects due to side walls, seasonal variations etc. In natural environments, studies of the effect of vegetation have mainly focused on the influence on resistance [8], which can be related to the blockage factor defined as the ratio of total frontal area of a vegetation to total area in the cross section. Most of these studies were conducted in marsh environments and open channels river type flows [30].

Artificial water conveyance systems may be considered as intermediate media between laboratory flumes and natural streams as they generally have a regular shape (similar to laboratory flumes) but also present some of the complexity of natural stream, with the presence of natural and non uniform vegetation. This vegetation may be composed of macrophytes, but smaller size colonies present in open channels, such as algal biofilms, may also affect velocity profiles, as studied in laboratory flumes [7, 14]. Field observations show that the development of such vegetation induced very large variations of roughness coefficients within short periods, causing serious management problems and large de viations of rating curves [16]. Vegetation can also alter velocity distributions, which may cause errors to flow measurements as a result of fitting standard velocity distributions to velocity measurements.

This paper aims to show how the growth of natural vegetation affects the parameters used to describe velocity profiles in real scale open channel flows. The first objective is to discuss the applicability of laboratory results to field conditions. The second objective is to analyze the seasonal variation of velocity profiles, and to show how the parameters of the velocity profiles are modified throughout the year.

The analysis is based on field measurements in a canal which conveys water con tinuously between March and October every year. In this canal, algae and macrophyte growth causes important management issues, such as clogging of hydraulic devices and substantial deviations of rating curves. After presenting the measurements, the validity of the modified log wake law (MLWL) [9] derived from laboratory flume experiments is then considered. Finally, the effects of vegetation growth on mean flow descriptors are discussed.

2 Materiel and methods

2.1 Experimental setup

The experimental work was carried out at two stations of the Gignac Canal, an open channel network which supplies water to 3000 ha of irrigated land in the south of France. The canal is operated between March and October, during which it supplies water for irrigation. During winter, the canal is closed, allowing maintenance works such as sedi ment and vegetation removal. The studied branch of the canal is designed to convey 1.5 m^3/s through a 15 km concrete canal. Two stations were selected, at strategic points where flow is measured for real time monitoring and control of the network. The two

stations have rectangular cross sections, and channel widths (denoted b) of 1.33 and 1 m, respectively. The local channel slopes, denoted S are equal to 0.0004 and 0.0013, re spectively. Water depth, denoted h, is monitored at a time step of 15 min by pressure transducers connected to a supervisory control and data acquisition system. At Station 1 (Fig. 1a), h varied between 0.65 and 1.325 m, and between 0.55 and 0.95 m at Station 2. On the channel side walls and on the bed, vegetation was mainly composed of bryophytes (*Fontinalis antipyretica*), a type of moss well adapted to the existence of dry periods. The plants consisted of small stems (up to a few centimeters long) and very small leaves (1 4 mm). The dry biomass was around 10 g/m^2 for both stations. At Station 1, macro phytes (mainly *Ranunculus fluitans*) grow during the irrigation season, and progressively dominate the bryophyte layer. The plant stems can grow to lengths of several meters in summer, but are bent by the flow and are completely submerged, occupying a layer of about 10 cm above the bed (Fig. 2). It was extremely difficult to measure the plant geometry within the flow, since this geometry varied with the season (stem length and foliage), and flow conditions (bending of the stem, strongly affecting the effective vegetation height in the flow, denoted h_p). Some pictures were taken under water, and plant samples were also collected, but the observed characteristics were hardly usable for de termining the relevant characteristics that could be used to predict velocity profiles. However, the influence of this vegetation could be clearly observed on velocity profiles (see Sect. 3.1). The influence of vegetation throughout the year was therefore observed thanks to regular sampling of velocity profiles, from which the effective vegetation height h_p was inferred.

Differences in vegetation types could be observed between the two stations. At Station 1, large macrophytes were observed mainly on the most insolated side (north side, i.e., $y \rightarrow b$), while macrophytes were smaller on the less insolated side. This caused consid erable heterogeneity in vegetation height, as can be observed from values of h_p at the same dates. Inversely, vegetation was fairly uniform on the bed of Station 2, which is oriented in the south north direction. For summer measurements, vegetation was slightly higher at the center of the channel ($y/b = 0.5$). This zone is also the most insolated of the channel, due to the orientation and the rather high banks of the channel (1.5 m, for a width of 0.8 m).

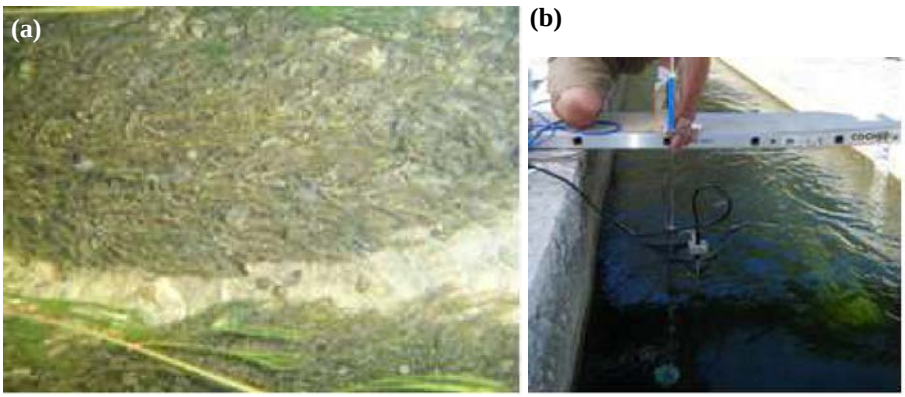

Fig. 1 Station 1, Gignac Canal (France), Lat: 43°42′33.12″N, Long: 3°33′20.84″E. Station 2 (43°40′36.39″N 3°32′42.35″E) has a similar shape. **a** Submerged vegetation, fixed on the canal bed (*Ranunculus fluitans*). **b** Micro ADV controller. View from the *upstream side* of the measurement section

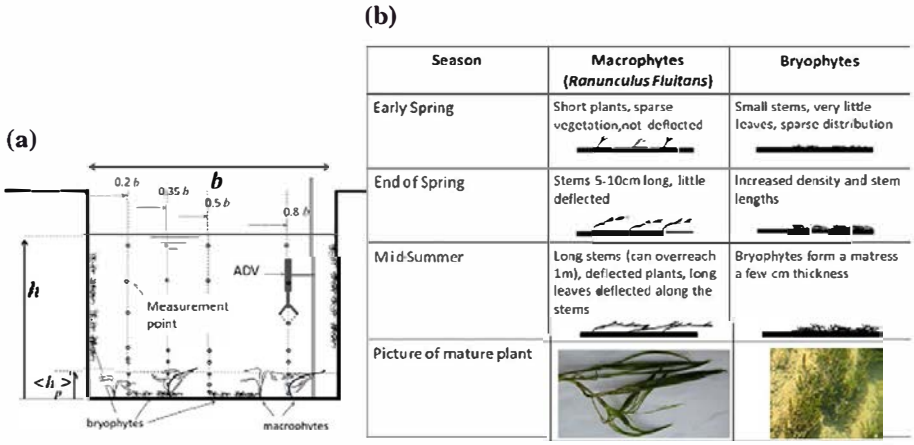

Fig. 2 Station 1, schematic description of the vegetation. a Lateral distribution of vegetation. b Evolution of the vegetation during the year

Two different series of velocity measurements were performed. The first one (denoted EM below) was carried out with an electromagnetic flowmeter (OTT *Nautilus* ™), with the objective of establishing rating curves at Stations 1 and 2 in different seasons between years 2000 and 2007. A total of 20 rating campaigns were conducted at each station. For each measurement of discharge, the velocity was measured at a minimum of 5 depths at least 7 points across the channel. These measurements of discharge were used to establish rating curves at each section. The temporal distribution of these measurements also allowed an analysis of the evolution of the velocity profiles in response to vegetation growth.

A second series of measurements (denoted ADV) was performed in 2010 in order to capture the evolution of roughness due to vegetation growth, and its effect on rating curves. For this purpose, measurements were taken about once a month between April and October 2010. The protocol was designed so that the vegetation height could be included as a parameter of the velocity profiles. Special attention was therefore needed for the flow in the logarithmic layer, where turbulence due to bed (and vegetation) roughness develops. These velocity measurements were performed using a 3D Vectrino micro ADV from Nortek™ (Fig. 1b) with an output rate of 25 Hz. The sample volume and transmit length were chosen

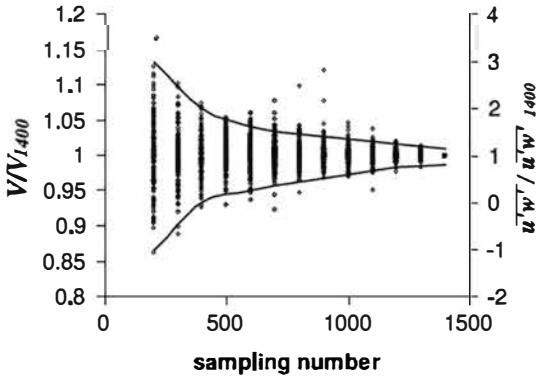

Fig. 3 Values of the longitudinal velocity and Reynolds stress as a function of the sampling number, normalized by the value estimated using 1400 samples. For the Reynolds stress results, only the standard error envelope (i.e., the distribution boundary) is plotted. All experimental measurements at the *centerline* (y 0.5b) were used

to ensure recommended measurement conditions, namely signal to noise ratio greater than 20, a sufficient amplitude signal, and correlation greater than 70 %. These conditions are obtained for a sample volume 1.9 mm high and a transmission length of 1.2 mm. For each point, the three velocity components were recorded during a minimum of 50 s (up to 56 s). This duration was chosen in order to establish velocity profile measurements over one day (constraint imposed by the operational management of the network), and to ensure a sufficient time convergence for the mean velocity. Four vertical lines were sampled ($y = 0.2b, 0.35b, 0.5b, 0.8b$, y transverse distance taken from left bank). At each vertical, the measurements were taken every 4 cm from the bed up to 24 cm, and every 12 cm up to the free surface. Reynolds stress was calculated using the second order velocity fluctuations.

To check the validity of the measurements, the sensitivity to the sampling number was studied (Fig. 3). A good convergence of the data was obtained for all the measurement points, yielding a standard error below 2 % for the longitudinal mean velocity and below 10 % for the Reynolds stress.

2.2 Parametrization of velocity profiles

Considering a rough open channel flow, the vertical velocity profile in the wall region follows the Prandtl logarithmic law modified by [23]:

$$\frac{u}{u_*} = \frac{1}{\kappa} \ln\left(\frac{z}{0.031 k_s}\right), \tag{1}$$

where u_* is the shear velocity, κ is von Karman's constant ($\simeq$0.41), z is the upward vertical coordinate taken from the bed, and k_s is the hydraulic roughness, found to be equal to the medium grain diameter for natural sediments. [29] presented a review of vegetated open channel studies based on log law formulation. They identified five methods for describing the velocity distribution. Comparing these methods, they concluded that it is difficult to provide a clear value for the parameters of Eq. (1).

In this study, the flow is separated conceptually in three layers to analyze the vertical velocity distribution. The first layer corresponds to the vegetated layer where the flow is influenced by the drag force exerted by the vegetation and the bed. The second layer is the free flow over the canopy. Several experimental studies showed that the velocity in the second layer can be expressed by a log law velocity profile similar to a turbulent boundary layer over roughness [11, 21]. Between these two layers, some authors propose to consider an intermediate zone which is similar to a mixing layer [1, 6]. However this approach is more appropriate for describing the vertical velocity distribution for low submergence and dense canopies [24], which was not the case here, since the ratio between water depth and canopy height was always greater than 10 in the channel. In our case, the velocity distribution is expected to be better represented by a boundary layer model. In the third layer, above the log law region, the velocity is influenced by secondary currents and the free surface. To represent the velocity in this layer, two terms can be added to the logarithmic profile, leading to the MLWL proposed by [9]. The main advantage that it correctly describes the dip phenomenon in open channel flows, i.e., the fact that the maximum velocity is under the water surface. In the experimental setup, this dip phenomenon can be very significant because of the substantial influence of the banks (size ratio b/h usually around 1). The log wake law is the one proposed by [2] up to the height h_m where velocity is maximum. The velocity over the canopy is expressed as follows:

$$u = \frac{u_*}{\kappa}\ln\left(\frac{z-d}{z_0}\right) - \frac{1}{3}\frac{u_*}{\kappa}\left(\frac{z-d}{h_\mathrm{m}-d}\right)^3 + \frac{2\Pi u_*}{\kappa}\sin^2\left(\frac{\pi(z-d)}{2(h_\mathrm{m}-d)}\right), \tag{2}$$

where d is the displacement height, z_0 is the hydraulic roughness, and Π is the wake strength parameter [9]. The displacement height (or zero plane displacement height), d, is the height at which the velocity would drop to zero if the logarithmic profile persisted within the vegetation. It represents the vertical shift of the logarithmic profile above the vegetation. The validity of such a formulation is analyzed further, and the way to set the values of u_*, z_0, d, h_m and Π will be discussed. To do so, calibration is performed step by step, starting from the lowest layer and ending with the upper region of the flow. In the lowest layer, corresponding to about 30% of the water column above the canopy, Eq. (2) reduces to Eq. (1) in which z is offset by d, and $z_0 = 0.031k_\mathrm{s}$. Using the measured velocities in this region gives access to u_*, z_0 and d. According to [11], z_0 and d are expected to be linked to the deflected plant height (h_p), also called "canopy height".

The analysis of the upper region gives the position of maximum velocity h_m. The dip phenomenon, expressed by the ratio $\delta = h_\mathrm{m}/h$, is expected to be affected by the banks. The experimental values of δ are compared to the experimental method proposed by [31]:

$$\delta = \frac{1}{1 + 1.3\exp(-y_\mathrm{b}/h)} \tag{3}$$

in which y_b is the minimal distance to the bank.

The wake strength parameter Π is known to be not universal. While the original paper by [2] suggested a value of $\Pi = 0.55$, [31] report values which are usually lower, and even negative, especially when the aspect ratio b/h is low [28]. Therefore, Π is calibrated on the field data, but values ranging from -0.15 to 0.55 were tested in the sensitivity analysis.

3 Hydrodynamic profiles

3.1 Mean velocity profiles

Figure 4 shows velocity contours at Sect. 1 for two depths in the same season (4a, b) and same depth but different seasons (4a, c). From these contours, three main regions can be

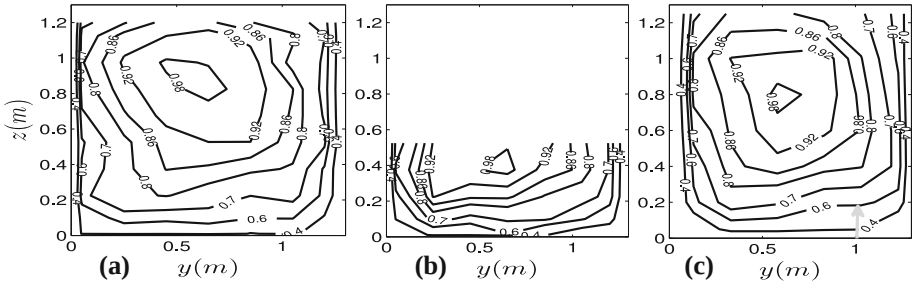

Fig. 4 Iso velocity contours of the relative longitudinal velocity (u/u_max) at Station 1: **a** $h = 1.23$ m, 4/20/2000 **b** $h = 0.55$ m, 3/4/2005, **c** $h = 1.25$ m, 6/24/2004. The *gray arrow* represents the position of deflected vegetation

identified: the turbulent boundary layer, mainly governed by the bottom shear stress (the first and second layers described above); the upper layer, with concentric contours centered around the point of maximum velocity, and the region near the bank, where the velocity is distributed in a fairly uniform manner, due to the wall roughness.

The turbulent boundary layer extends over the lower third of the section ($z \in [0; \simeq 0.3h]$). In this domain, velocity contours are mostly horizontal, which means that there is little variation of velocity with lateral position. This is explained by the fact that velocity profiles are driven by the bed properties, with the result that a standard logarithmic distribution should be appropriate to describe the variation of mean velocity with depth.

The comparison of Fig. 4a and c illustrates the effect of bed vegetation. These profiles are taken in spring and summer, respectively. The gray arrow on Fig. 4c represents the location of a macrophyte affecting the velocity distribution. The isoline $u = 0.6U_{\max}$ is located higher in summer than in spring because of the presence of longer macrophytes on the right side which causes some heterogeneity of bed roughness (Fig. 4c). Similar results are observed at Station 2. As another illustration of the effect of vegetation, Fig. 5 shows velocity profiles at the centerline in spring and summer 2010, measured at the same water depths. The displacement of the logarithmic zone is clearly observed near the bed, while the depth averaged velocity is reduced by about 10 %.

In the upper part, velocity profiles are also influenced by secondary currents due to the side walls. This causes the maximum velocity to be located under the surface (between about 0.6 and $0.8h$), which is referred to as the dip phenomenon. This phenomenon is clearly linked to the aspect ratio of the section (Fig. 4). When h is small, which is the case in spring (Fig. 4b), the maximum velocity is observed close to the surface. On the other hand, when h is large, the maximum velocity is reached at a lower ratio of the total depth, about half of it in the most extreme case.

The discharge is calculated by integrating the velocities in both the y and z directions. For the z direction, the measurement density is usually sufficient to allow the use of linear interpolation. Alternatively, the MLWL can also be used, as described below. For the transverse distribution of velocities (y axis), it is preferable to fit a typical velocity dis tribution. This was established with the EM measurements, where the highest density of

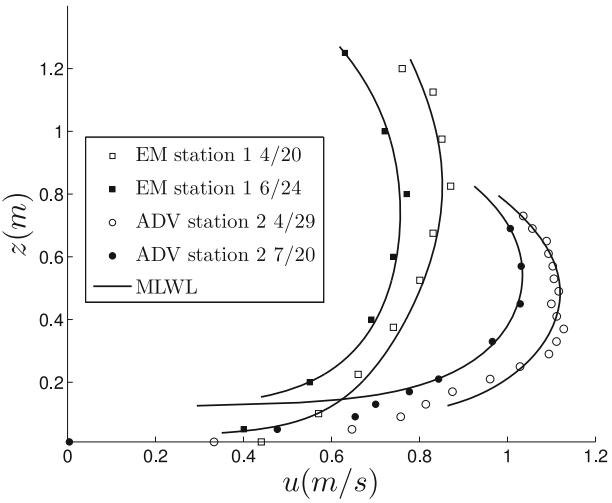

Fig. 5 Vertical velocity profiles at the channel centerline, for same water depths in spring (*open signs*) and summer (*full signs*). The *solid lines* represent the MLWL fitting from Eq. (2). Displacement height depends on the season

measurements was taken. For this purpose, the layer influenced by the vegetation patch was excluded by considering only the velocity for points where $z > 0.4h$. Figure 6 shows the ratios of mean velocities in verticals ($u(z)$) to the mean velocity at the centerline, as a function of relative distance from the banks, for all measurements. A classic power law could be found for the lateral distribution:

$$\frac{u(z)}{U_c(z)} = \left(\frac{y_b}{b/2}\right)^{\frac{1}{m}}, \tag{4}$$

where $U_c(z)$ is the velocity at the centerline and at the vertical abscissa z, y_b is the minimal distance to one bank (left or right), and m is a coefficient depending on side wall roughness. A value of $m = 7$, corresponding to smooth side walls, fits well to the measured velocities. This is consistent with the fact that the vegetation is less developed on the side wall. The sensitivity of the discharge to this coefficient is analyzed below (see Sect. 3.4).

3.2 Velocity fluctuations

From the second order velocity fluctuations u' and w', in the longitudinal and vertical directions x and z, respectively, the Reynolds stress can be calculated for each measure ment as follows:

$$\tau_{xz} = -\rho\overline{u'w'} \tag{5}$$

in which ρ is the water density.

The vertical profiles of the Reynolds shear stress $-\rho\overline{u'w'}$ reach a maximum close to the bed (Fig. 7a). As shown in previous studies [17, 27, 32], the position of this maximum corresponds to the top of the submerged canopy, denoted h_p. Since this point is far enough from the bottom, the viscous stress is small, so this maximum is very close to the total shear stress ρu^{*2}. Therefore, for each vertical profile sampled with ADV, the values of h_p and u_* could be identified from the vertical profiles of Reynolds stresses. To reduce errors due to the time convergence and the vertical sampling (4 cm step), the vertical profiles of τ_{xz} are fitted with a spline function. Figure 7a illustrates the normalized profiles of Rey nolds stresses, plotted on the same graph for both stations with all available measurements. The results are consistent with those obtained in laboratory conditions [6, 21].

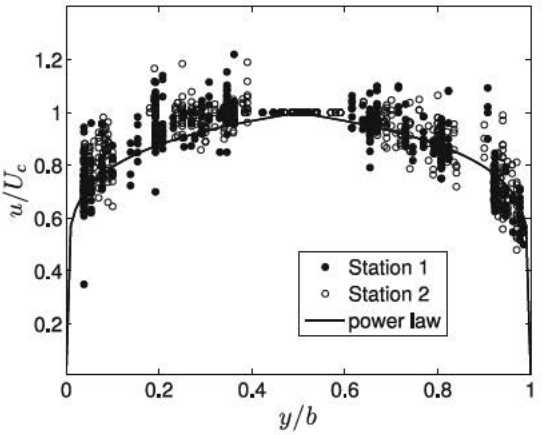

Fig. 6 Transverse distribution of the velocity at Stations 1 and 2 for EM measurements. U_c is the centerline velocity at a given vertical position. The *solid line* represents the power law fitting from Eq. (4)

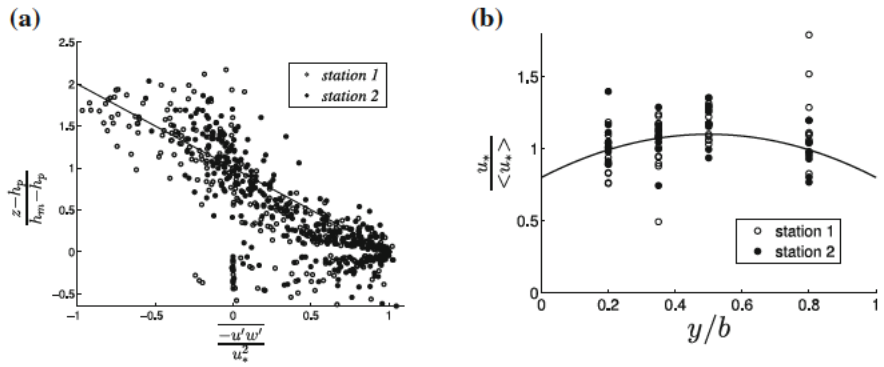

Fig. 7 Distribution of shear stress and shear velocity, all ADV measurements (Stations 1 and 2). **a** Vertical distribution of the normalized Reynolds stress. **b** Transverse distribution of the shear velocity, Stations 1 and 2

For each station, the lateral distribution of the shear velocity is analyzed by comparing the local values of u_* with the weight averaged lateral value $\langle u_* \rangle$. Figure 7b reveals that the shear velocity decreases near the walls, as expected, due to friction on side walls. Some heterogeneity of vegetation can explain higher values than $\langle u_* \rangle$ near the wall. Nevertheless, the local shear velocities do not deviate greatly from the average value, so the transverse variability is rather limited. This is in accordance with the remark about the velocity contours in the lower part of the flow.

Other methods can be used to determine u_*. Following [22], u_* could also be fitted from the first order velocity variations in the logarithmic layer. Conversely, we show below that u_* obtained from Reynolds stress gives an accurate description of the logarithmic layer. By considering the total momentum variation in a canal reach, one can then link the local shear stress to the slope of energy line as follows:

$$\langle u_* \rangle \simeq \sqrt{g R_\mathrm{h} S} \tag{6}$$

with g the acceleration due to gravity, $R_\mathrm{h} = (h - h_\mathrm{p})b/(2(h - h_\mathrm{p}) + b)$ the hydraulic ra dius (calculated by excluding the vegetated area), and S the slope of energy line. When the flow is uniform, S is the bed slope (S_b) which is constant over time, but this situation is rare in real systems due to geometry and flow changes, as well as hydraulic structures causing backwater effects. Flow cannot be assumed to be uniform for both stations, except at higher flow. For laboratory experiments with no side friction, [22] remarked that the friction velocity obtained from the energy slope was greater than that obtained from local measurements.

3.3 Experimental parameters of the velocity profiles

Near the canopy, the logarithmic term in Eq. (2) is predominant. The logarithmic layer requires the determination of u_*, d, and z_0. The determination of d and z_0 is quite chal lenging, since no universal rule applies to vegetated beds, although it is admitted that both are linked to the height of vegetation. [11] suggested considering roughness height as equal to the vegetation height in Eq. (1), which is equivalent to consider $z_0 = 0.031 h_\mathrm{p}$ and $d = 0$. Although this may apply to sparsely vegetated beds, several experimental studies

concluded that these relationships should be adapted in the case of dense canopies , while experimental results exhibit quite large dispersion for the ratios z_0/h_p [3, 13, 18].

In order to obtain these ratios, h_p and u_* are determined from second order velocity fluctuations as explained previously. In a second step, h_p and u_* are used to determine d and z_0 from the logarithmic term in the MLWL (Eq. 2), considering only the measurements within the layer $z \in [h_p; h_p + 0.3h]$, where the contribution of the wake can be ignored. The parameters of the MLWL are adjusted by minimizing the quadratic error between Eq. (2) and the experimental values (simplex method, *fminsearch* function from Matlab). Figure 8 demonstrates that the velocity profile is logarithmic in this region.

Figure 9 shows the variation with h_p of the displacement height and hydraulic rough ness, both normalized by h_p. The variations of these coefficients are consistent with the results obtained by [17] ($0.01 \langle z_0/h_p \rangle 0.5$). [12] proposed an analytical model to estimate d/h_p and z_0/h_p over a vegetated bed. Their model requires the vegetation density and area, which are unknown in our case. However, with an assumed constant frontal area ($a = 1.2\,\mathrm{m}^{-1}$), the agreement between model and experiments is good and the variation with h_p is correctly reproduced. The low value of z_0/h_p corresponds to higher h_p, *i.e.*, to isolated macrophytes which are not representative of the averaged vegetation height. Constant ratios $d/h_p = 0.75$ and $z_0 = 0.01 h_p$ give a good estimation.

The upper part of the flow is now analyzed. Two parameters, δ and Π, are needed to calculate the wake function, expressed by the last two terms in Eq. (2). When a large number of measurements are available in the upper region, δ can be obtained directly from the measurements. Alternatively, δ and Π can be adjusted simultaneously on the wake functions (Eq. 2), using all data between h_p and h for each velocity profile with the optimization function. Figure 10 shows the variation of δ as a function of b/h. In most cases, parameter δ is clearly lower than 1, due to the influence of the side walls. The measurements are in good agreement with the expression proposed by [31]. This is also consistent with the results of [9] for rough flow over gravel beds.

Calibrating the wake strength parameter Π for each vertical profile leads to values between -0.3 and 0.6. The negative values are obtained with almost uniform velocity distributions near the side walls, whereas Π varies between 0.05 and 0.6 elsewhere. The

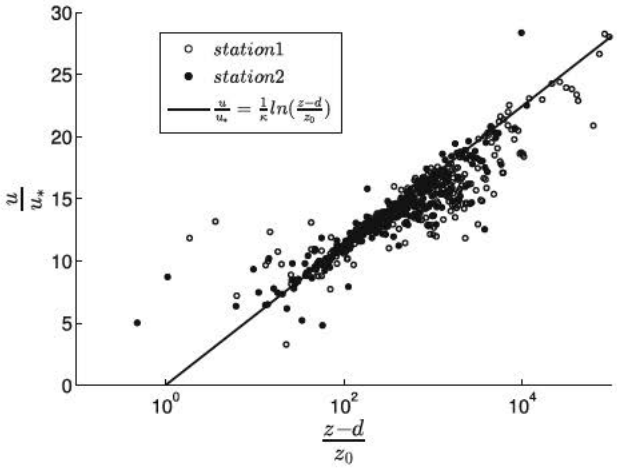

Fig. 8 Velocity profile at each *vertical line* for ADV measurements

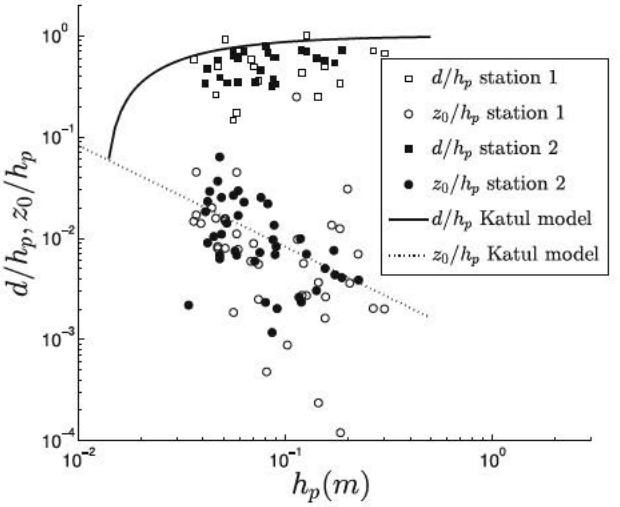

Fig. 9 MLWL parameters from ADV measurements with Π 0 (*line*)

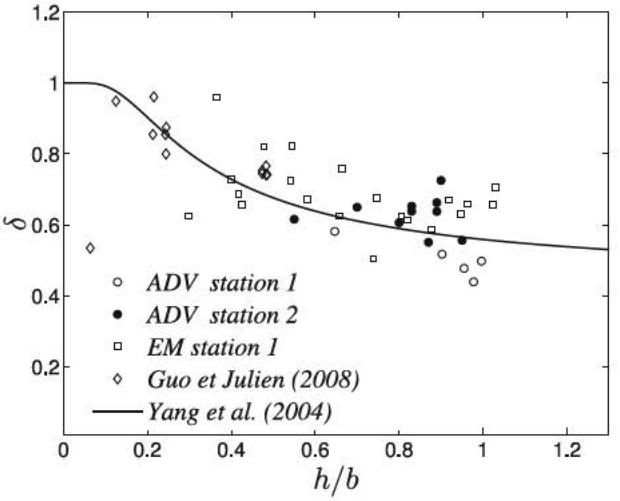

Fig. 10 Height of maximum water velocity as a ratio of water depth (δ h_m/h) as a function of the aspect ratio b/h

value of 0.2 proposed by [20] is within this range. A constant value $\Pi = 0.2$ for all profiles remains acceptable. In particular, a change of Π has a limited effect on the bulk velocity. This point is discussed below.

3.4 Sensitivity to the MLWL parameters

For a given section, the vertical velocity profile at the centerline, denoted U_c, is deduced from the MLWL while the transverse distribution is given by Eq. (4). A unique shear

velocity, $u_* = \langle u_* \rangle$ is used, which can be calculated from Eq. (6) for instance. The total discharge Q is given by

$$Q = 2 \int_d^h U_c \int_0^{b/2} \left(\frac{y}{b/2} \right)^{\frac{1}{m}} \mathrm{d}y\mathrm{d}z \tag{7}$$

Considering $h \gg d$, the integration gives [9]:

$$Q = \frac{u_*}{\kappa} \quad \log\left(\frac{h}{z_0}\right) - \frac{\Pi}{\pi}\delta \sin\left(\frac{\pi}{\delta}\right) - \frac{1}{12}\left(\frac{1}{\delta}\right)^3 + \Pi - 1 \Bigg) \frac{m}{m+1} b \tag{8}$$

To study the sensitivity of the discharge to all the parameters, including those describing the vegetation, a reference state Q_0 is chosen by taking $d/h_\mathrm{p} = 0.75$ and $z_0/h_\mathrm{p} = 0.01$, $\delta = 0.7$, $\Pi = 0.2$, $m = 7$, $h = 1$ m, $h_\mathrm{p} = 0.05$ m. The effect of changing h_p, δ, Π, and m is observed on the total discharge (Fig. 11a d). The ranges of variation are defined by the observed ranges of variation for all experiments.

The most sensitive parameter is h_p (Fig. 11a). An increase of h_p by 10 cm causes a dramatic decrease of the discharge (almost 20 %), while a very small vegetation height (1 cm) results in a discharge increased by 20 %. The second most influential parameter is m. For rough side walls, m can reach 5, while it can reach values of 7 or more for smooth walls. In the case of rough walls ($m = 5$), the error regarding discharge is then less than

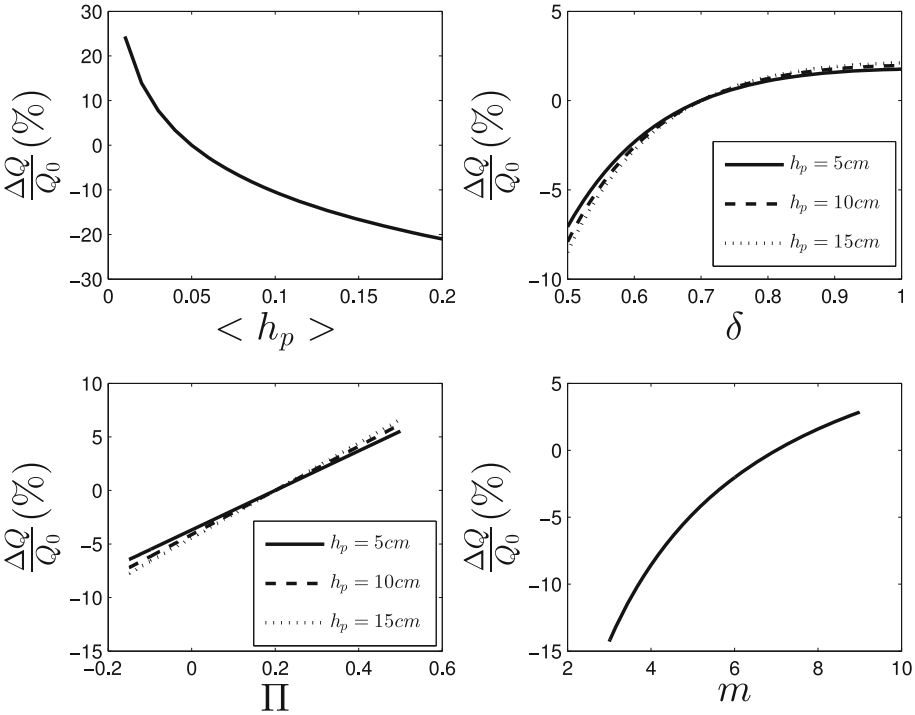

Fig. 11 Sensitivity of the total discharge with the MLWL and m parameters

10 %. This result significant, however, and suggests that wall friction should be considered carefully, particularly when width to depth ratios are small, as is the case for both stations.

From Fig. 11b, c, it can be concluded that the choice of Π and δ has a relatively limited influence on discharge (less than 5 %), compared to the effect of vegetation height. In order to study the effect of vegetation, these parameters are considered as a constant. Note also that assuming $h \gg d$ (leading to Eq. 8), and zero velocity inside the vegetation, leads to an error on discharge lower than 5 %.

4 Seasonal influence of vegetation

The purpose of this study is to show how vegetation growth modifies rating curves. We demonstrate below the effect of variations in h_p on rating curves and Manning's roughness coefficients.

At the beginning of the year, canals are quite clean, as most of the vegetation is removed during winter when canals are closed. Most of the vegetation remaining on the bed consists of bryophytes, only a few centimeters high. During spring, macrophytes start growing and reach their maximum length in summer, between 30 and 50 cm on average. Some filamentous algae (although not present at both stations) may even grow to lengths of one meter and more. This vegetation is bent under the action of the flow, so the actual plant height is much lower than the total plant length. As described previously, the deflected plant height is extremely difficult to measure directly, but it can be determined from the velocity profiles.

Considering $d/h_p = 0.75$ and $z_0 = 0.01 h_p$ as constant, as observed for ADV measurements, the same parameters are applied to EM velocity profiles, and h_p and u_* are determined from the measurements in the logarithmic layer ($z \in [0.1; h_p + 0.3h]$) using the MLWL and the simplex method. By using EM measurements it is possible to exploit a larger data set with a wide span throughout the year.

The y averaged values of $\langle h_p \rangle$ are plotted in Fig. 12, for all available measurements (EM and ADV), as a function of the days of the year. It reveals that h_p exceeds 10 cm in August

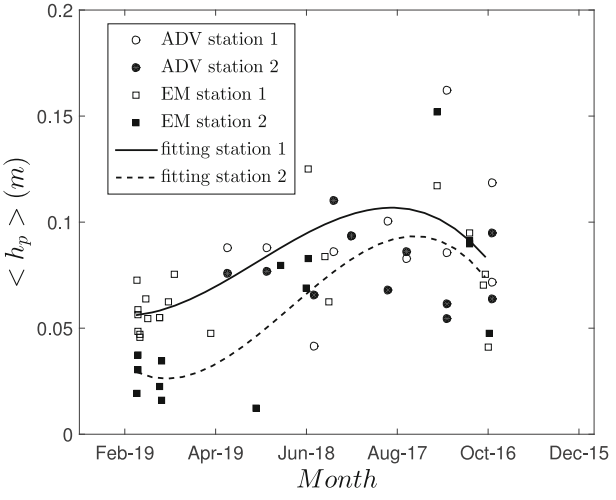

Fig. 12 Seasonal distribution of the averaged deflected vegetation height $\langle h_p \rangle$ estimated from measurements with the ADV and EM instruments. EM measurements were taken between 2000 and 2006, and ADV measurements during the year 2010. *Lines* represent 3rd order polynomial interpolation

at both stations, which is consistent with direct field observations. Growth of h_p is observed until July, after which it decreases continuously until October.

The friction forces exerted on the bed and plants can be calculated using the local shear velocities. For higher water levels, the flow in the canal tends to be uniform, while both stations are under backwater effects at low flow. Therefore, when R_h increases, shear velocities should tend toward $u_{*b,unif} = \sqrt{gR_hS}$ (friction velocity calculated in uniform flow). Figure 13 shows the variation of the normalized shear velocities $\langle u_* \rangle / u_{*b,\mathrm{unif}}$ with hydraulic radius that tend to 1 when R_h is large. This means that u_{*b}, the mean bottom shear stress calculated at the reach scale, is consistent with the mean local shear stress, calculated from local velocities. [22] observed that u_{*b} was about 1.6 times larger than $\langle u_* \rangle$ in their rectangular laboratory flume. Calculating u_{*b} using water depth instead of hydraulic radius (for example, excluding the friction due to the side walls) would give about the same value.

Manning's equation is the most frequently used approach to calculate the friction head loss at reach scale, from which stage discharge relationships can be derived. The seasonal evolution of $\langle h_p \rangle$ requires the choice of varying Manning coefficients throughout the year, which is possible using the MLWL. Considering $\langle u_* \rangle = u_{*b}$, Manning's coefficient n is linked to the velocity profile as follows:

$$n = \frac{\langle u_* \rangle bh}{Q\sqrt{g}} R_h^{1/6} \tag{9}$$

in which Q is given by Eq. (8). For all measurements, n was calculated as above, using the computed discharge and the experimental values of h, R_h, $\langle u_* \rangle$, and $\langle h_p \rangle$. To take account of the dip phenomenon, Yang et al.'s formula was used to calculate δ, while m was set to 7 and Π to 0.2. The obtained Manning coefficients varied between $n = 0.015$ and $n = 0.026$ s/m$^{1/3}$ (Fig. 14). Note that the Manning coefficients can be calculated for each measurement campaign using the measured discharge ($n_{\mathrm{experimental}}$), or the discharge calculated from Eq. (8) using $\langle h_p \rangle$ which simulates the regular growth of vegetation throughout the year.

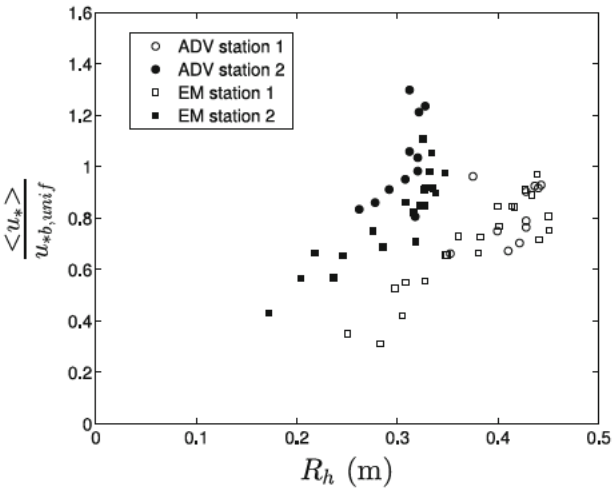

Fig. 13 Shear velocity as a function of the hydraulic radius at the 2 stations

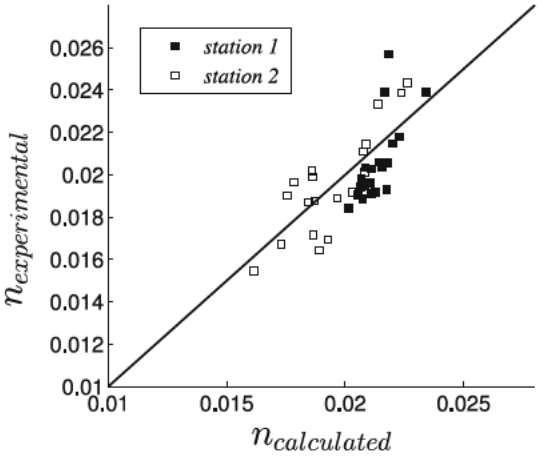

Fig. 14 Computed Manning roughness coefficient

The simulated values of n (with Eq. (8) and $\langle h_p \rangle$) are used to build rating curves using Manning's equation, taking account of backwater effects with actual field measurements of the channel geometry. To this end, a one dimensional model of the Gignac Canal [15] was used with steady condition and with constant Manning coefficients in the longitudinal direction. These rating curves are compared to those obtained from field measurement campaigns (Fig. 15), established with EM measurements and used to operate the Gignac Canal. A good agreement between curves is found. This means that the use of the MLWL, and the method applied to parameterize it, is relevant for analyzing the effect of vegetation throughout the year.

The advantage is that the evolution of h_p can be estimated. Also, a continuous evolution of h_p is expected at different periods, so interpolated values may be used to re construct rating curves at different dates as illustrated in Fig. 15. In our case, the rating curve evolved continuously between the two limits defined by the extreme values of n. A consequence for canal operation is that a given measured water level corresponds to different discharges

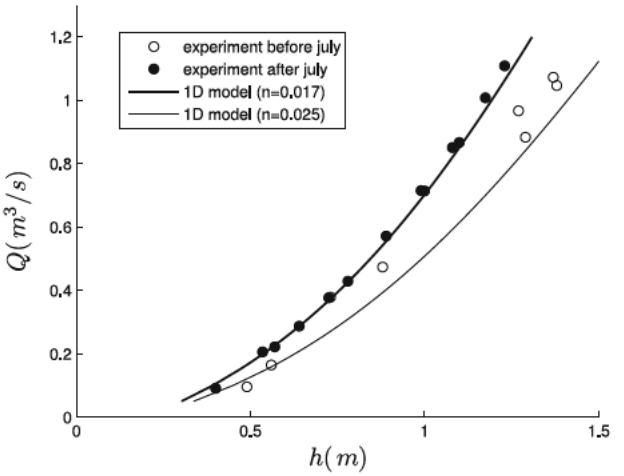

Fig. 15 Rating curve at Station 1

according to the date of the year. Here, it can be seen that the deviation of the rating curve reached 25 % between the beginning of the year and summer (Fig. 15).

5 Conclusion

This study attempted to assess the validity of the MLWL, established under laboratory conditions, for a real scale channel with natural vegetation. The second objective was to analyze the seasonal variations of velocity profiles in response to vegetation growth. To do so, two sites were selected in an operational irrigation canal affected by vegetation growth. The following conclusions can be drawn from this study:

ADV measurements can be used to determine the shear velocity and the deflected vegetation height, as previously shown in laboratory studies, using either mean velocity distribution in the logarithmic layer or the Reynolds stress profiles.
The MLWL describes the velocity profiles with a good accuracy (error less than 5 %). The values found in laboratory tests are confirmed for δ and Π, while h_p and z_0/h_p are the most sensitive parameters.
Velocity profiles evolve throughout the year, due to vegetation growth and senescence. By taking a constant ratio for z_0/h_p, knowing the value of h_p allows the evolution of velocity profiles to be determined, with more integrative parameters such as Manning roughness coefficients. This, in turn, means that rating curves can be generated at any moment of the year.

Future research should focus on the best way to estimate h_p from direct measurements, taking account, among other factors, of plant characteristics, plant flow interaction, and heterogeneity (different macrophytes and vegetation patches). Some of this heterogeneity, essential for studies in natural streams, can also be found in man made canals which are easier to investigate.

References

1. Carollo FG, Ferro V, Termini D (2002) Flow velocity measurements in vegetated channels. J Hydraul Eng 128(7):664 673
2. Coles D (1956) The law of the wake in the turbulent boundary layer. J Fluid Mech 1:191 226
3. Defina A, Bixio A (2005) Mean flow and turbulence in vegetated open channel flow. Water Ressour Res 41:1 12
4. Ghisalberti M, Nepf HM (2002) Mixing layers and coherent structures in vegetated aquatic flows. J Geophys Res 107(2):1 11
5. Ghisalberti M, Nepf HM (2004) The limited growth of vegetated shear layers. Water Resour Res, 40(7)
6. Ghisalberti M, Nepf HM (2006) The structure of the shear layer in flows over rigid and flexible canopies. Environ Fluid Mech 6:277 301
7. Graba M, Moulin FY, Boultreau S, Garabtian F, Kettab A, Eiff O, Snchez Prez JM, Sauvage S (2010) Effect of near bed turbulence on chronic detachment of epilithic biofilm: experimental and modeling approaches. Water Resour Res, 46(11)
8. Green JC (2006) Effect of macrophyte spatial variability on channel resistance. Adv Water Resour 29(3):426 438
9. Guo J, Julien P (2008) Application of the modified log wake law in open channels. J Appl Fluid Mech 1(2):17 23
10. Huai W, Zeng Y, Xu Z, Yang Z (2009) Three layer model for vertical velocity distribution in open channel flow with submerged rigid vegetation. Adv Water Resour, 32(4), 487 492. Cited By (since 1996) 3

11. Jarvela J (2005) Effect of submerged flexible vegetation on flow structure and resistance. J Hydrol 307(1 4):233 241
12. Katul GG, Poggi D, Ridolfi L (2011) A flow resistance model for assessing the impact of vegetation on flood routing mechanics. Water Resour Res, 47(8)
13. Klopstra D, Barneveld H, van Noortwijk J, van Velzen E (1997) Analytical model for hydraulic resistance of submerged vegetation. In: Proceedings of the 27th IAHR congress, pp 775 780
14. Labiod C, Godillot R, Caussade B (2007) The relationship between stream periphyton dynamics and near bed turbulence in rough open channel flow. Ecol Model 209(2 4):78 96
15. Litrico X, Malaterre PO, Baume JP, Vion PY, Ribot Bruno J (2007) Automatic tuning of PI controllers for an irrigation canal pool. J Irrig Drain Eng 133(1):27 37
16. Lozano D, Dorchies D, Belaud G, Litrico X, Mateos L (2012) Simulation study on the influence of roughness on the downstream automatic control of an irrigation canal. J Irrig Drain Eng 138(4):285 293
17. Luhar M, Rominger J, Nepf H (2008) Interaction between flow, transport and vegetation spatial structure. Environ Fluid Mech 8:423 439. doi:10.1007/s10652 008 9080 9
18. Nepf H, Ghisalberti M (2008) Flow and transport in channels with submerged vegetation. Acta Geophys 56:753 777
19. Nepf HM (2012) Hydrodynamics of vegetated channels. J Hydraul Res 50(3):262 279
20. Nezu I, Nakagawa H (1993) Turbulence in open channel flows. Balkema, The Netherlands
21. Nezu I, Sanjou M (2008) Turburence structure and coherent motion in vegetated canopy open channel flows. J Hydro environ Res 2(2):62 90
22. Nikora N, Nikora V, O'Donoghue T (2013) Velocity profiles in vegetated open channel flows: com bined effects of multiple mechanisms. J Hydraul Eng 139(10):1021 1032
23. Nikuradse J (1933) Laws of flow in rough pipes (in translation, naca tm 1292, 1950). VDI Forschungsheft
24. Pietri L, Petroff A, Amielh M, Anselmet F (2009) Turbulent flows interacting with varying density canopies. Environ Fluid Mech 9(3 4):297 320
25. Plew DR, Cooper GG, Callaghan FM (2008) Turbulence induced forces in a freshwater macrophyte canopy. Water Resour Res, 44(2)
26. Raupach MR, Antonia RA, Rajagopalan S (1991) Rough wall turbulent boundary layers. Appl Mech Rev 44(1):1 25
27. Righetti M (2008) Flow analysis in a channel with flexible vegetation using double averaging method. Acta Geophys 56(3):801 823
28. Roussinova V, Biswas N, Balachandar R (2008) Revisiting turbulence in smooth uniform open channel flow. J Hydraul Res 46(supp 1):36 48
29. Stephan U, Gutknecht D (2002) Hydraulic resistance of submerged flexible vegetation. J Hydrol 269(1 2):27 43
30. Sukhodolov A, Thiele M, Bungartz H (1998) Turbulence structure in a river reach with sand bed. Water Resour Res 34(5):1317 1334
31. Yang S, Tan S, Lim S (2004) Velocity distribution and dip phenomenon in smooth uniform open channel flows. J Hydraul Eng 130(12):1179 1186
32. Yang W, Choi S U (2009) Impact of stem flexibility on mean flow and turbulence structure in depth limited open channel flows with submerged vegetation. J Hydraul Res 47(4):445 454